DØ- CONF note 4574

Measurement of the Top Quark Mass in the Lepton+Jets Channel using DØ Run II Data

The DØ Collaboration
URL: http://www-d0.fnal.gov

(Dated: August 12, 2004)

In this note, we present measurements of the top quark mass, using lepton+jets events collected in $p\overline{p}$ collisions at $\sqrt{s} = 1.96$ TeV at the Fermilab Tevatron using the DØ detector. The dataset corresponds to an integrated luminosity of approximately 160 pb^{-1} collected between April 2002 and November 2003. We use two different methods for measuring the top quark mass using a kinematic fitting technique. One method uses Templates of signal and background mass spectra to determine the top quark mass. The second method is based on the Ideogram technique and calculates an analytical likelihood for each event. The event likelihood takes into account all possible jet assignments and the probability that an event was signal or background. We measure the top quark mass to be in the range: $m_t = 170.0 \pm 6.5(\text{stat})\,^{+10.5}_{-6.1}\,(\text{syst})$ GeV and 177.5 ± 5.8 (stat) $\pm$ 7.1 (syst) GeV, depending on the assumption on the background model, where the first number is from the Template method using constrained background fit and the second is from the Ideogram method using a background un-constrained fit.

Preliminary Results for 2004 Summer Conferences

I. INTRODUCTION

One of the main goals of Run II of the Fermilab Tevatron is the detailed study of the top quark. The top quark was discovered by the DØ and CDF collaborations in 1995 during Run I of the Tevatron [1]. In Run I the two experiments each accumulated an integrated luminosity of about 100 pb^{-1}. From these data measurements of the top pair production cross section and the top quark mass were obtained.

The measurement of the top quark mass is interesting because it is an important parameter in many predictions of the Standard Model. In particular, precise knowledge of the top quark mass, together with the W boson mass, constrain the mass of the Higgs boson in the framework of the Standard Model. The measurement of the top quark mass by the DØ collaboration from Run I data is 179.0 ± 5.1 GeV [2],[3].

Here we present the first measurements of the top quark mass from Run II data by DØ. The integrated luminosity used for this measurement is about 160 pb^{-1}. We present measurements from the lepton+jets channel using two different methods. The "Template" method is very similar to the technique used for the first top quark mass measurement by DØ [3]. The "Ideogram" method applies some ideas used by the DELPHI Collaboration for the W boson mass measurement [5] to our measurement of the top quark mass.

The top quark decays to a W boson and a b quark. The W boson can either decay to leptons ($e+\nu_e$, $\mu+\nu_\mu$, $\tau+\nu_\tau$) or quarks (ud', cs'). The quarks will manifest themselves as jets in our detector. If the W bosons from the top decays to $e\nu$ or $\mu\nu$ and the W boson from the antitop decays to quarks (or vice versa), the events contain one charged lepton and four jets (from the two b quarks and the W). We call this the lepton+jets channel. It is characterized by a sizeable branching fraction ($\approx 30\%$) and small backgrounds. Events of this type kinematically constrain the top quark mass. We do not use events in which the W decays to $\tau\nu$ because they are harder to identify and reconstruct.

II. COMMON DATA SET AND SELECTION

The data sample used is the same as for the topological cross section analysis in the lepton+jets channel. The first step is to identify events in which have a high p_T electron or a muon accompanied by substantial $\not\!\!E_T$, indicative of a W boson production in the final state. We require isolated electron (muon) candidates to have $p_T > 20$ GeV, be within the pseudorapidity range $|\eta| < 1.1$ ($|\eta| < 2.0$) and to satisfy tight quality requirements. The muon p_T is also required to not exceed 150 GeV. A minimum event $\not\!\!E_T$ of 20 GeV (17 GeV) is required for the e+jets (μ+jets) events. Next, we select events with at least 4 jets with transverse momentum $p_T > 15$ GeV, out of which the leading 3 jets are required to have a $p_T > 20$ GeV. The jets must all be in the pseudorapidity range $|\eta| < 2.5$.

The dominant source of background is production of a W boson, which decays to $e\nu$ or $\mu\nu$, and several light-quark and gluon jets. The jets in these events tend to be softer than the jets from top decays. The p_T cuts in the selection are designed to reduce this background. Another, much smaller, source of background is from multijet events where one of the jets is misidentified as a lepton and have significant p_T imbalance due to detector resolution. In the μ+jets channel, muons from heavy flavor quark decays can fake isolation if the hadronic activity in the unreconstructed jet fluctuates low. Jets can be mis-identified as electrons when there is a leading π^0 that overlaps with the track of a charged particle and muons can originate from the decay of π and K mesons. These mis-identification background sources are minimized by requiring that the missing energy is acollinear with the lepton direction. To further reduce the background from mis-identified electrons in multijet events, we require that $E_T^W = \left|p_T^l\right| + |\not\!\!E_T| > 65$ GeV.

A final selection on the kinematic fit of the event to the $t\bar{t}$ hypothesis is applied (see section III). We require that at least one jet permutation which fits the top quark decay hypothesis has a $\chi^2 < 10$. This requirement keeps 96% of the $t\bar{t}$ events and further reduces the W+jets (multijet) background by 7%(10%).

The numbers of events that pass this selection are shown in Table I, together with the estimated sample composition.

Channel		e+jets	μ+jets
Number of Events		101	90
Sample Composition	$t\bar{t}$	30.9	29.9
	W + jets	65.7	53.4
	multijets	4.4	6.9

TABLE I: Number of events passing the event selection and breakdown in signal and background contributions from the cross section analysis.

III. KINEMATIC CONSTRAINED FIT

Both analyses use a kinematic constrained fit to extract mass information from the events. The fit technique is the same as used in the Run I Template analysis [3]. The object resolutions used in the fit were updated to reflect those of the Run II DØ detector.

The events are reconstructed using the measured momenta of the charged lepton and the four jets with the highest p_T and the missing transverse momentum. In addition to these 17 measured numbers, three constraints can be imposed. The invariant mass of the decay products of the two W bosons must equal the W boson mass and the invariant mass of the two Wb pairs must be equal. Since we need 18 numbers to completely define the six-particle final state we can perform a 2-C fit to the top-antitop decay hypothesis. There are 12 possible ways to assign the four jets to the b and $\overline{b}$ quarks and the two quarks from the decay of the W boson. The fit routine considers all 12 permutations and for each permutation returns a best fit top quark mass and a fit χ^2.

IV. MASS SPECIFIC JET ENERGY SCALE CORRECTIONS

Due to fragmentation and detector effects, the measured energy in a jet cone is not equal to the energy of the original parton. Thus the jet energies have to be calibrated before we can measure the top quark mass.

The first step in calibrating the jet energy scale is to correct the measured energy of the jets to be equal on average to the energy of the particles in the jet cone. This is done in the same way for data and events from Monte Carlo simulation so that both are on equal footing. The measured jet energy (E_{meas}) is corrected using the following expression:

$$E_{corr} = \frac{E_{meas} - O}{R \times S},$$

where R is the calorimeter response (determined requiring p_T balancing in γ+jets events). O is the energy offset due to the underlying event, energy pile-up, multiple interactions, electronic noise and uranium noise from the uranium absorber. O is determined from energy densities in minimum bias events. S is the fraction of shower energy that remains inside the jet cone ($\Delta R = 0.5$) in the calorimeter and is determined from the measured energy profiles of jets. These corrections are applied to all jets.

In addition, jets originating from b quarks (b jets) may contain a lepton from the semileptonic decay of the original B hadron and in this case the jet does not include the energy of the escaping neutrino. In the case of an electron all the energy of the lepton will be contained in the calorimeter jet, while for a muon only a small amount of energy is deposited (typically on the order of 2 GeV). Thus for semileptonic decays to muons the energy of the b jet is corrected for the muon energy and the energy of the neutrino and the correction factor is derived using Monte Carlo samples of b-quark semileptonic decays.

The second step is to correct the energy of the jets to equal on average that of the original parton. Determining this parton-level correction requires knowledge of the parton momentum 4-vector and the reconstructed jet momentum. It can therefore only be determined from simulated Monte Carlo events. The parton-level corrections are derived as a function of energy for jets originating from the fragmentation of light quarks (u, d, s, c) and heavy quarks (b), and in three pseudorapidity bins. Using the information from the generated events, the primary partons from $t\bar{t}$-decay (before radiation) are matched to jets. Only uniquely matched jet-parton pairs are used to avoid biasing the corrections by the occasional hard gluon radiation that generates two distinct jets or overlap of jets from two or more partons.

This is the same procedure as used in reference [3].

V. LOW BIAS DISCRIMINANT

In order to get further discrimination between signal and background, we derive a discriminant (Low Bias Discriminant, LB) constructed from the topology of the events. Because of the large mass of the top quark, $t\bar{t}$ events have a unique topology. The discriminant is designed to be uncorrelated with the top quark mass. We developed this discriminant by closely following the work described in reference [3].

The four topological variables considered here are:

1. The reconstructed $\not\!\!E_T$.
2. $\mathcal{A} \equiv \frac{3}{2} \times$ smallest eigenvalue of $\mathcal{P}$

3. $H'_{T2} \equiv \frac{H_{T2}}{H_{\parallel}}$

4. $K'_{Tmin} \equiv \frac{(min\ of\ 6\ \Delta R_{ij}) \cdot E_T^{lesser\ j}}{E_W^T}$

$\mathcal{A}$ is the aplanarity of the event and $\mathcal{P}$ is the normalized momentum tensor of the event derived from the momenta of the jets and the reconstructed W boson. It is defined by:

$$\mathcal{P}_{ij} \equiv \frac{\sum_a p_{a,i} p_{a,j}}{\sum_a |\vec{p}_a|^2}, \tag{1}$$

where i and j label the spatial components of the momentum, and a runs over all jets and the reconstructed W boson. $\mathcal{A}$ is defined as $\frac{3}{2}$ times the smallest eigenvalue of $\mathcal{P}$ and has a range of 0 to 0.5. It can be shown [4] that the decay products from a massive particle have large values of aplanarity.

$H_{\parallel}$ is the scalar sum of $|p_z|$ of the jets, isolated lepton, and the neutrino. H_{T2} is the scalar sum of the $|p_T|$ of the jets excluding the leading jet. H'_{T2} gives rather good discrimination and has only a small correlation with the fit mass. Although variables such as H_T have notably better discrimination power, Run I experience showed that the correlation with the fit mass was unacceptably large [3].

K'_{Tmin} is a measure of the jet separation folded together with "transverse energy" of the reconstructed leptonic W boson. ΔR_{ij} is the distance between jet i and jet j in $\eta - \phi$ space. Of the six possible ΔR_{ij} between the four leading jets, the smallest is chosen. $E_T^{lesserj}$ is the smaller of the two jet E_T's.

The distributions for the individual variables are shown in Fig. 1. The likelihood is constructed by the procedure described in [3]. The discriminant is shown for signal and background in Fig.2.

An alternative way to reduce the background in the sample is to require one or more of the jets to be tagged as b jets. In Fig. 3 we show the low bias discriminant versus fitted mass for our data sample and for the subset of events that have a b jet. It is obvious that the b-tagged events (which are enriched in top signal) cluster at larger values of the discriminant. This demonstrates the power of the discriminant to distinguish signal and background.

VI. THE TEMPLATE MASS ANALYSIS

A. Method for mass extraction

The Template analysis is based on comparing the fitted mass from the kinematic fit on the collider data with the results obtained from fitting simulated Monte Carlo data samples of known top masses. In this comparison we use the fitted top quark mass from the permutation with the smallest χ^2 as the mass estimator. We apply the same event selection on the Monte Carlo events as on the collider data. For each hypothetical top quark mass, we create templates by constructing a histogram of fit masses with 10 GeV wide bins from 80 to 280 GeV. We also construct a background template from the most prominent background to our decay channel: W + 4 jet production.

In order to extract the top quark mass from this comparison, we use a binned likelihood fit. We write the probability distribution function for the mass estimator in terms of the number of signal events n_s and the number of background events n_b in our sample. We constrain the fraction of background events to the expected number using a Poisson probability term.

For each hypothesized top quark mass, the likelihood is maximized as a function of the number of signal and background events. The mass with the largest likelihood, or equivalently the smallest negative log likelihood ($-\ln(L)$) is identified and a parabola is fit to the values of $-\ln(L)$ for all hypothesized top quark masses within $\pm$ 15 GeV of the mass with the largest likelihood. The minimum of the parabola is taken as the most likely top quark mass and the statistical uncertainty is extracted by finding the mass for which the fit to $-\ln(L)$ rises by $\frac{1}{2}$.

To extract the most likely number of signal events, we interpolate between the values of n_s at the two top quark masses which straddle the minimum of the fit to $-\ln(L)$.

B. Performance on MC

In order to test our method of measuring the top quark mass, we performed a series of simulated Monte Carlo experiments. For these we fit ensembles of Monte Carlo events in the same way as the collider data. The size of each ensemble was fixed to the total number of events seen in data. The mean fraction of signal and background was adjusted to agree with the fit to the collider data sample. However, in each ensemble the number of $t\bar{t}$ events and background events were allowed to vary according to binomial statistics. These ensemble tests were performed in order to evaluate

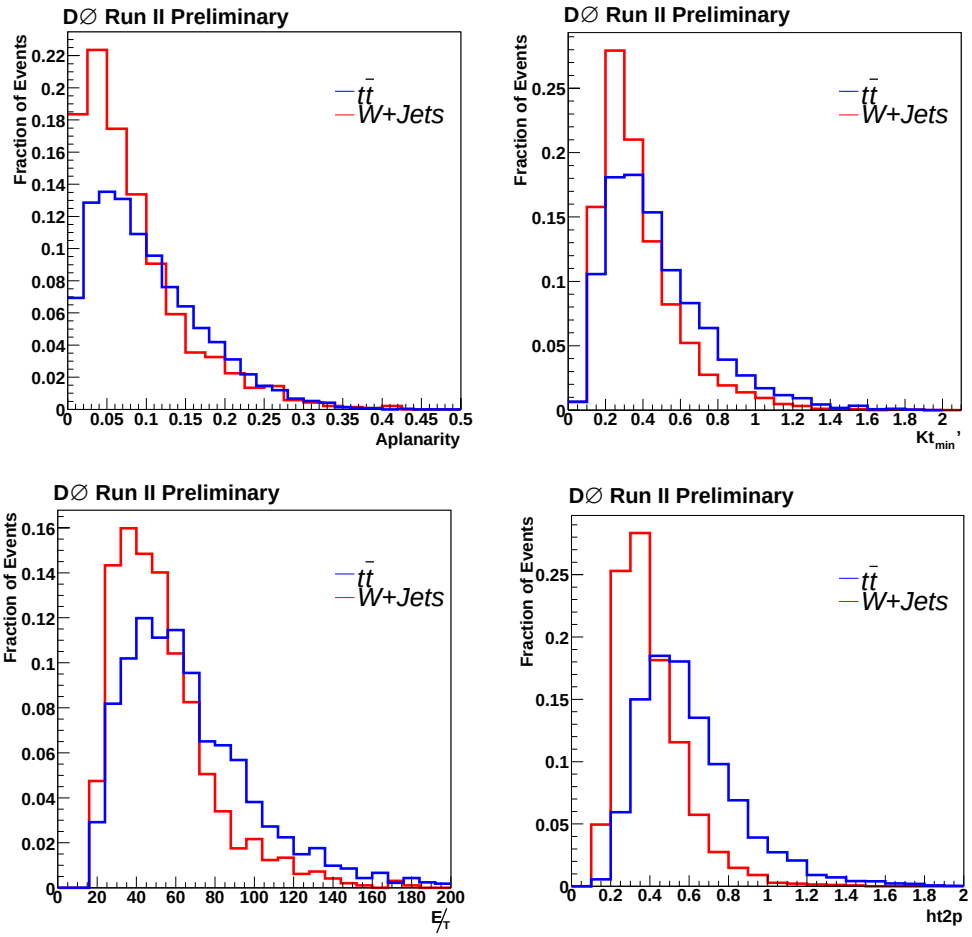

FIG. 1: $\mathcal{A}$ distributions (top left), K'_{Tmin} distributions (top right), $\not\!\!E_T$ distributions (bottom left) and H'_{T2} distributions (bottom right) for $t\bar{t}$ and background.

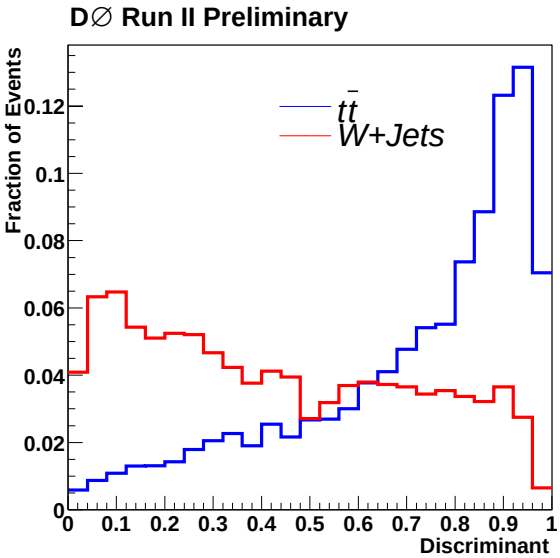

FIG. 2: Low Bias Discriminant

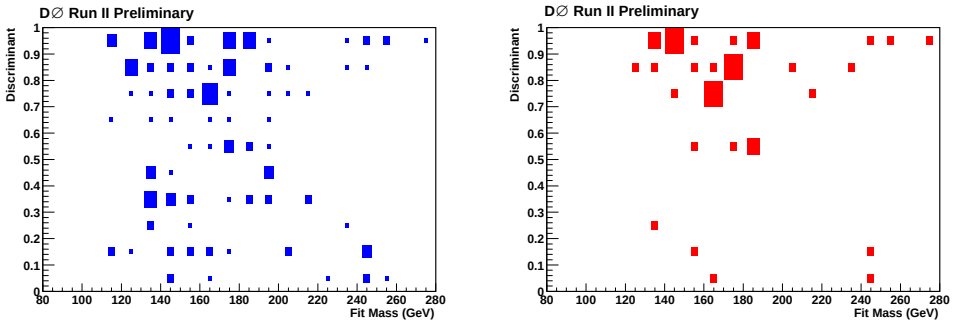

FIG. 3: Low Bias Discriminant versus fitted mass for the events in the collider data sample. The left plot (solid blue boxes) is for all events in our sample and the right plot (solid red boxes) shows the subset of events that are b-tagged.

the calibration of the method, the expected statistical uncertainty, and to verify that the uncertainties assigned by the fit are consistent with the statistical spread of the ensembles. The results shown in Figs. 4 6 demonstrate that the method is well calibrated and assigns uncertainties that are consistent with the statistical spread seen in the ensembles. These results are also summarized in Table II.

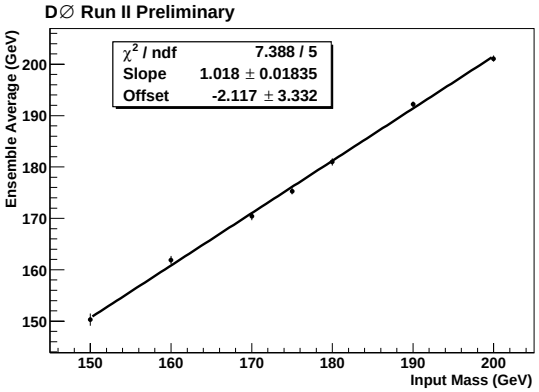

FIG. 4: Calibration of Template fitting method. The points show the correlation between the input top quark mass to the output mass from the fit. The result of the fit to the points (line shown) is consistent with a slope of one and an offset of zero.

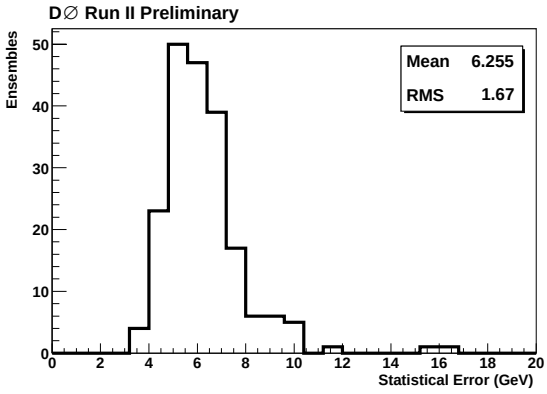

FIG. 5: Distribution of the expected statistical uncertainty from ensemble tests for an input top quark mass of 170 GeV.

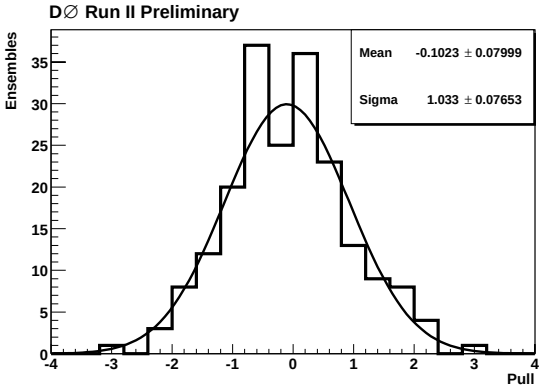

FIG. 6: Distribution of the pull from ensemble tests for an input 170 GeV top quark mass. The superposed curve is a to a Gaussian with width ≈ 1 and mean of zero.

TABLE II: Means and Pulls of ensemble tests for various input top quark masses.

Input Mass	Average Output Mass	Width of Gaussian Fit to Pull
150 GeV	150.3 ± 1.2 GeV	0.96 ± 0.07
160 GeV	161.9 ± 0.8 GeV	1.02 ± 0.05
170 GeV	170.4 ± 0.8 GeV	1.03 ± 0.07
175 GeV	175.3 ± 0.7 GeV	0.99 ± 0.05
180 GeV	181.0 ± 0.7 GeV	0.95 ± 0.06
190 GeV	192.2 ± 0.5 GeV	0.96 ± 0.06
200 GeV	201.1 ± 0.6 GeV	0.99 ± 0.07

C. Mass measurement from collider data

In addition to the selection described in section II, we apply a cut on the low bias discriminant D and on H_{T2}. Only events with $D > 0.4$ and $H_{T2} > 90$ GeV are used for the Template fits. This selection retains 83% of the $t\bar{t}$ events while rejecting about 70% of the W+jets and multijet backgrounds. After this final event selection we find 87 events in the lepton+jets channel. The fit mass distribution of the events is shown in Fig. 7. The fit for the top quark mass is shown in Fig. 8. The topological cross-section analysis, with the slight differences in event selection taken into account, predicts that 40 of the 87 events are background. We fit a top quark mass of

$$m_{\rm t} = 170.0 \pm 6.5 \text{ GeV (stat)}$$

with 38 ± 8 $t\bar{t}$ events (statistical uncertainties only).

D. Systematic uncertainties

We considered several sources of systematic uncertainty on the measurement. The uncertainties considered were: the jet energy scale, the jet energy resolution, modeling of the underlying event, trigger bias, limited Monte Carlo statistics, calibration uncertainty, and the $t\bar{t}$ model in the MC.

The dominant systematic uncertainty originates, as expected, from the jet energy scale. This was evaluated by scaling the jet energy scale up and down by 1σ for both the signal and background Monte Carlo samples. The uncertainty on the jet energy scale has been conservatively taken to be 5% for jet $E_T > 30$ GeV. These events were then used in ensembles and fit using templates with the nominal jet energy scale. The difference in the mean top mass obtained from these ensembles and the ensembles with the nominal energy scale was taken as the uncertainty associated with the jet energy scale calibration. This resulted in a variation of $+9.0$ GeV and -4.0 GeV.

The jet energies in the Monte Carlo events were smeared to more closely model the detector performance. This smearing was varied by $\pm 1\sigma$ in both signal and background Monte Carlo events and ensemble tests repeated using templates with the nominal jet energy resolution. The resulting variation, $+3.0$ and -1.5 GeV, was taken to be the systematic uncertainty for the jet energy resolution.

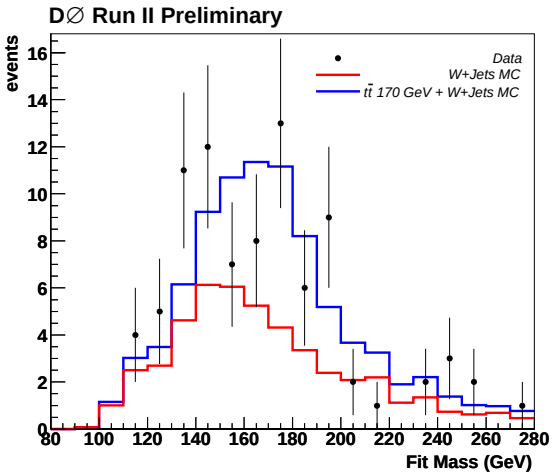

FIG. 7: The fit mass distribution of final event selection. As well, the signal and background mass distributions are shown in the fraction that is preferred by the fit.

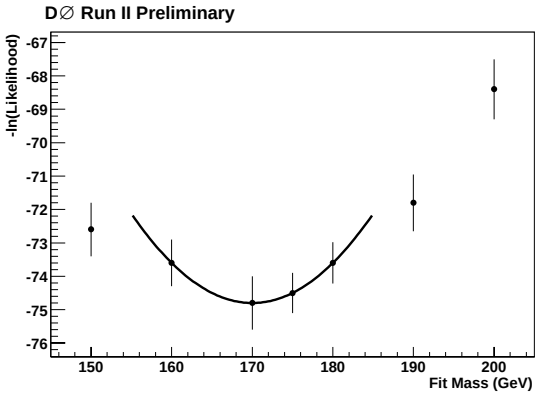

FIG. 8: $-\ln(L)$ distribution as a function of the fit top quark mass. The background constrained fit yields a top quark mass of 170.0 $\pm$ 6.5 GeV (statistical) in the lepton + jets data sample.

Almost all of our Monte Carlo samples were generated with the underlying event generation disabled. Only one special sample was generated with the correct underlying event included in the event generation. From this sample we composed ensembles and fit them using templates without the underlying event and the resulting variation is quoted as a systematic uncertainty of 3 GeV.

Since there is a finite number of Monte Carlo events, statistical fluctuations in the signal and background templates can lead to an uncertainty in the extracted top mass. In order to quantify this effect we divided the Monte Carlo sample into four subsamples to produce four different sets of background and signal templates. Then ensembles were produced from the full Monte Carlo set and fit with the four sets of signal and background templates. In this case the ensembles formed were fixed and the templates sets were varied. The uncertainty was computed as the rms of the results from the four sets of templates divided by the square root of the number of different templates $\sqrt{N-1}$ (e.g $N = 4$ here) to account for the fact that we have four times the number of events in our templates. The result is an uncertainty of 0.5 GeV.

Although the calibration curve is consistent with zero offset and unit slope, there is of course point to point variation in the calibration curve. We take the parameters from the fit calibration along with the uncertainties and compute the uncertainty which is associated with the uncertainty in the calibration curve. This procedure produces an uncertainty of 0.5 GeV

We simulate the effect of trigger efficiencies by removing events from the ensembles by throwing a random number and comparing it to the probability for that event to satisfy the trigger. This is done for all the Monte Carlo templates. In order to ascertain the uncertainty associated with a possible trigger bias, we prepare Monte Carlo ensembles in which the trigger efficiency is not taken into account. To be conservative, we take the uncertainty to be twice the

Source	Uncertainty
Jet Energy Scale	-4.0 $+9.0$ GeV
Jet Energy Resolution	± 2.3 GeV
Underlying Event and Multiple Interactions	$+3.0$ GeV
Limited MC Statistics	± 0.5 GeV
Trigger Uncertainty	± 1.0 GeV
Calibration Curve	± 0.5 GeV
$t\bar{t}$ Model	± 3.8 GeV
total	-6.1 $+10.5$ GeV

TABLE III: Systematic Uncertainties. This Table shows the variation of the top mass that is seen when various quantities which enter the top mass estimation are varied with in $\pm 1\sigma$ of there known values.

observed change in the average output mass and quote an uncertainty of 1.0 GeV.

The uncertainty from the $t\bar{t}$ model is taken from the Run I top quark mass measurement and increased by a factor two to cover possible differences in the analyses.

The systematic uncertainties are summarized in Table III. After adding the uncertainties in quadrature we measure the top quark mass to be

$$m_{\rm t} = 170.0 \pm 6.5({\rm stat}) \, ^{+10.5}_{-6.1} ({\rm syst}) \ {\rm GeV}$$

VII. THE IDEOGRAM ANALYSIS

The second analysis uses an approach very similar to the Ideogram technique that was used by the DELPHI experiment [5] to measure the mass of the W boson at LEP. The mass information from the kinematic constrained fit is used to construct an event likelihood taking into account all possible jet permutations. The low bias discriminant D is used on an event-by-event basis to estimate the probability that an event is background. Therefore no cut on D is necessary and it was omitted to improve the statistical sensitivity. Similarly, no cut on H_{T2} was deemed necessary. Finally, the overall fraction of signal events in the event sample was allowed to float freely in the likelihood fit.

A. Method for mass extraction

The kinematic fit is the same as the one used by the Template method. The difference is that all information from the kinematic fit is taken into account. It is used to construct an event likelihood $\mathcal{L}_{\rm evt}(m_{\rm t}, P_{\rm samp})$ as a function of the top mass $m_{\rm t}$ and overall $t\bar{t}$ fraction in the sample $P_{\rm samp}$. For each event 12 possible jet combinations are considered, and for each combination up to two different starting guesses for the p_z of the neutrino are considered. In about 60% of parton-matched e+jets $t\bar{t}$ events at 175 GeV (55% in the muon+jets channel), considering both starting guesses for the neutrino in the 'correct' jet combination leads to two identical fitted masses. In 20% it leads to different top mass solutions that are less than 5 GeV apart. In the remaining 20% of the cases (25% in the muon+jets channel) it yields two mass solutions that differ by more than 5 GeV. Whether or not the mass values are different, two masses per jet combination are included in the likelihood. Thus each event yields 24 masses m_i, uncertainties σ_i and χ^2_i values indicating the goodness-of-fit. A relative probability of each jet assignment w_i is calculated as

$$w_i = \exp(-\frac{1}{2}\chi^2_i)$$

If for a particular jet permutation both neutrino solutions i and $i+1$ fail to converge, the corresponding weights w_i and w_{i+1} were chosen to be zero. However, if for a particular jet permutation only one of the two neutrino solutions leads to a converging fit, that solution is used twice for consistency with other jet combinations. Also the probability for the event to be signal $P_{\rm evt}$ is estimated (see below) and the likelihood to observe this event is calculated as follows:

$$\mathcal{L}_{\rm evt}(m_{\rm t}, P_{\rm samp}) = P_{\rm evt} \cdot \left[\int_{100}^{300} \sum_{i=1}^{24} w_i \cdot \mathbf{G}(m_i, m', \sigma_i) \cdot \mathbf{BW}(m', m_{\rm t}) dm' \right] + (1 - P_{\rm evt}) \cdot \sum_{i=1}^{24} w_i \cdot {\rm BG}(m_i)$$

The signal term consists of a convolution of the sum of the Gaussian resolution functions $\mathbf{G}(m_i, m', \sigma_i)$ describing the experimental resolution with a relativistic Breit-Wigner $\mathbf{BW}(m', m_{\rm t})$, representing the expected distribution of the average of the two invariant masses of the top and anti-top quark in the event, for a top mass $m_{\rm t}$. The background term consists of the weighted sum $\mathrm{BG}(m_i)$, where BG(m) is the shape of the mass spectrum from W+4 jet and multijet events observed in MC simulation. The Breit-Wigner and background shape are both normalized to unity on the integration interval: 100 to 300 GeV. This interval was chosen large enough not to bias the mass in the region of interest. The sensitivity to the signal fraction $P_{\rm samp}$ in the sample enters through the estimated event purity $P_{\rm evt}$, which depends on $P_{\rm samp}$ and on the value of the topological discriminant D for that event, in the following way:

$$P_{\rm evt} = \left(\frac{S}{S+B}\right)_{\rm evt} = \frac{(S/B)_{\rm evt}}{(S/B)_{\rm evt}+1} = \frac{(S/B)_{\rm samp}\cdot(S/B)_D}{(S/B)_{\rm samp}\cdot(S/B)_D+1}$$

where

$$(S/B)_{\rm samp} = \frac{P_{\rm samp}}{1-P_{\rm samp}}$$

and $(S/B)_D$ is derived from the estimated event purity $P(D)$, parameterized as a function of the discriminant value D for a sample with a S/B ratio equal to unity.

$$(S/B)_D = \frac{P(D)}{1-P(D)}$$

Since each event is independent the combined likelihood for the whole sample is calculated as the product of the single event likelihood curves:

$$\mathcal{L}_{\rm samp}(m_{\rm t}, P_{\rm samp}) = \prod_j \mathcal{L}_{{\rm evt}j}(m_{\rm t}, P_{\rm samp})$$

This likelihood is maximized with respect to the top mass $m_{\rm t}$ and the estimated fraction of signal in the sample $P_{\rm samp}$.

B. Performance on MC

The analysis must be calibrated using MC simulation. Both the bias on the measured mass and the correctness of the estimated statistical uncertainty can be tested using ensemble testing, where each ensemble represents a simulated experiment corresponding to the size of the data sample observed in data. Thousands of ensembles were constructed, combining $t\bar{t}$ and W+jets from MC and multijet events obtained from data by requiring reversed lepton isolation cuts. The fractions of $t\bar{t}$, W+jets and multijet were allowed to fluctuate according to multinomial statistics around the estimated fractions in the actual data sample. The fractions used are listed in Table I. The total sample size was fixed to the observed number of events in data (101 in e+jets and 90 in μ+jets). To make optimal use of the available MC statistics standard re-sampling techniques were used, allowing for the multiple use of MC events when constructing the ensembles.

Figure 9 shows how the mass bias and width of the pull vary as a function of the generated mass. In Figure 10 the bias on the mass and width of the mass pull are shown as a function of the generated purity, varying the signal fraction in the samples from 0.1 to 0.9. The reliability of the mass fit is remarkable over the whole range of purities and masses tested.

The expected statistical sensitivity as a function of the mass, including all corrections, is shown in Fig. 11. For a top mass of 175 GeV, the expected statistical uncertainty is 6.2 GeV in the e+jets channel, 6.5 GeV in the μ+jets channel, and 4.6 for both channels combined (using the sigma of the Gaussian fit to the ensemble mass distribution, divided by the calibration slope).

C. Mass measurement from collider data

The likelihood curves as a function of the top mass are shown in Fig. 13. The mass thus extracted from the likelihood is: 178.1 ± 10.2 GeV in the e+jets channel, 178.7 ± 9.0 GeV in the μ+jets channel, and 178.4 ± 6.8 GeV in the combined channel. The RMS of the pull shown in Fig. 12 was used to correct the estimated uncertainty in the

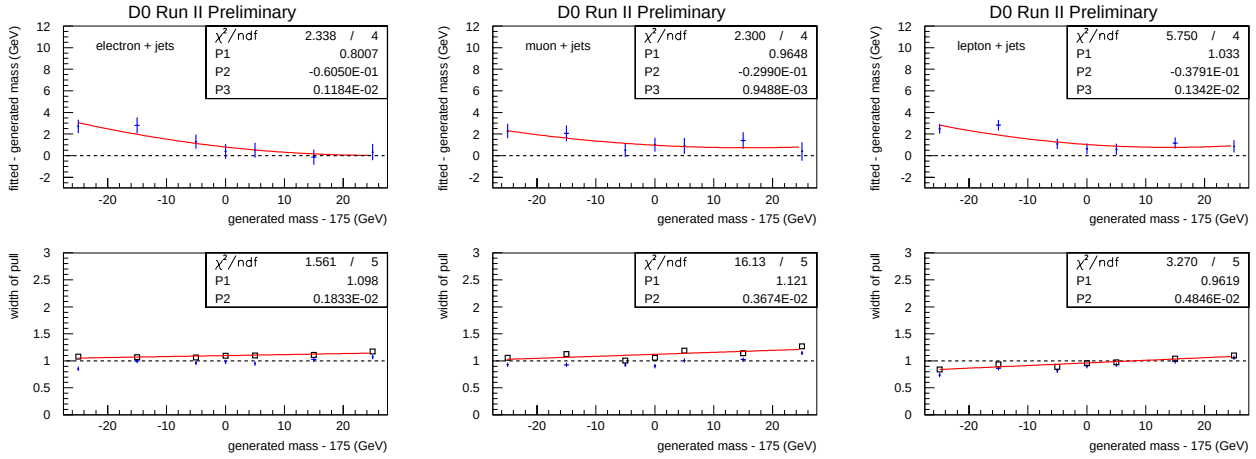

FIG. 9: Mass bias (= fitted mass - generated mass) as a function of the generated mass and width of the pull as a function of the generated mass, for e+jets (left), μ+jets (middle) and both channels combined(right). The RMS of the pull, indicated with the square boxes, is sometimes larger than the sigma of a fit to the pull distribution, indicated with the points with error bars.

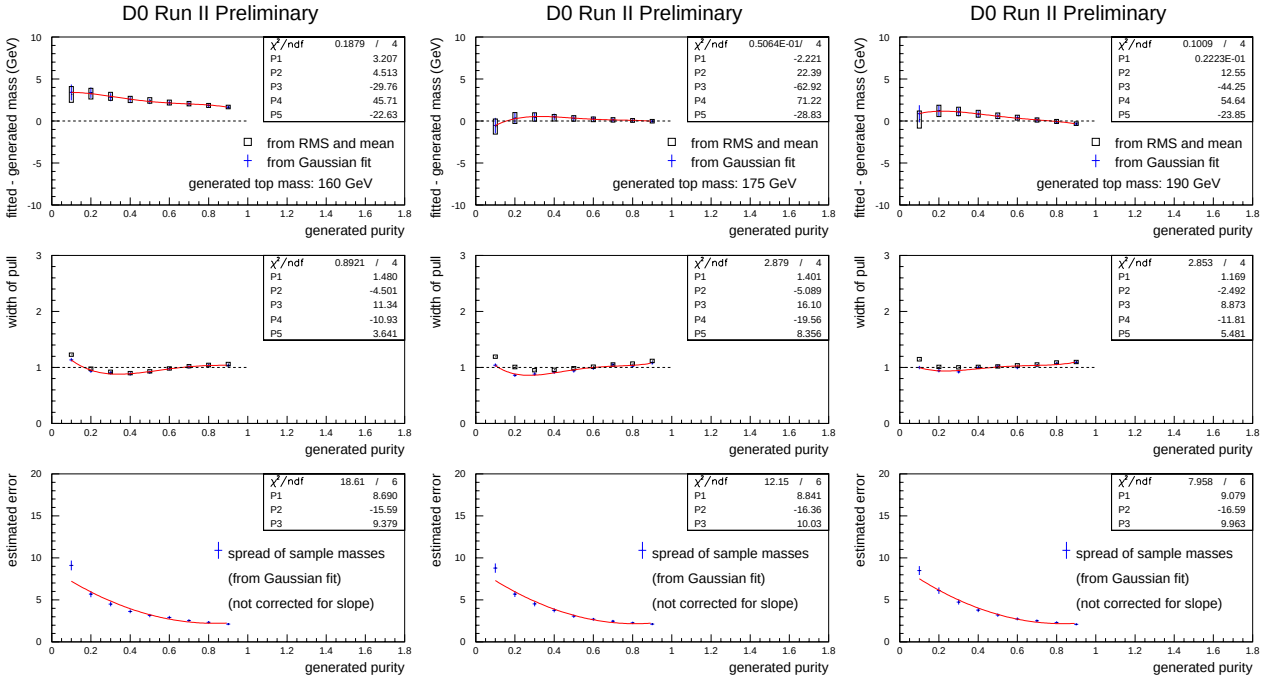

FIG. 10: Average mass bias (top), width of the mass pull (middle) and expected uncertainty on the mass (bottom) as a function of the signal fraction in the ensembles, for three different values of the generated top mass.

analysis, in addition to a correction for the calibration slope. After correction for the calibration curve and RMS of the pull distribution the results are:

$$m_{\rm t} = 177.6 \pm 11.9 \text{ (stat) GeV}$$

for e+jets, and

$$m_{\rm t} = 177.8 \pm 9.5 \text{ (stat) GeV}$$

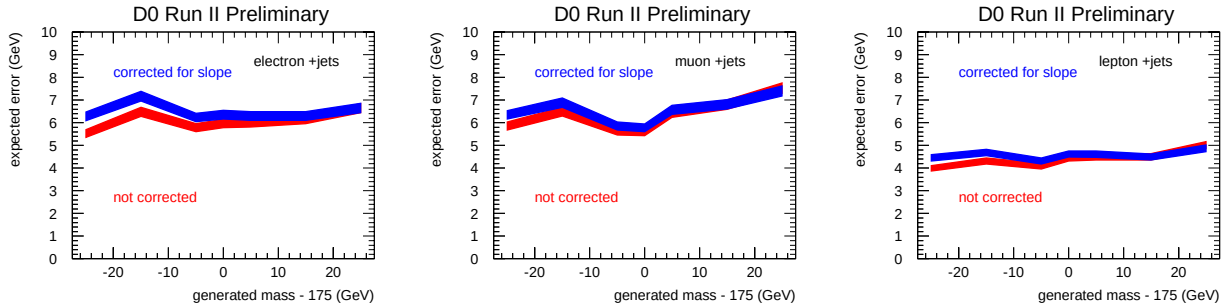

FIG. 11: Expected statistical mass sensitivity (= sigma of Gaussian fit to ensemble mass distribution / calibration slope) as a function of the generated top mass, for the e+jets channel (left), the μ+jets channel (middle) and the two channels combined (right).

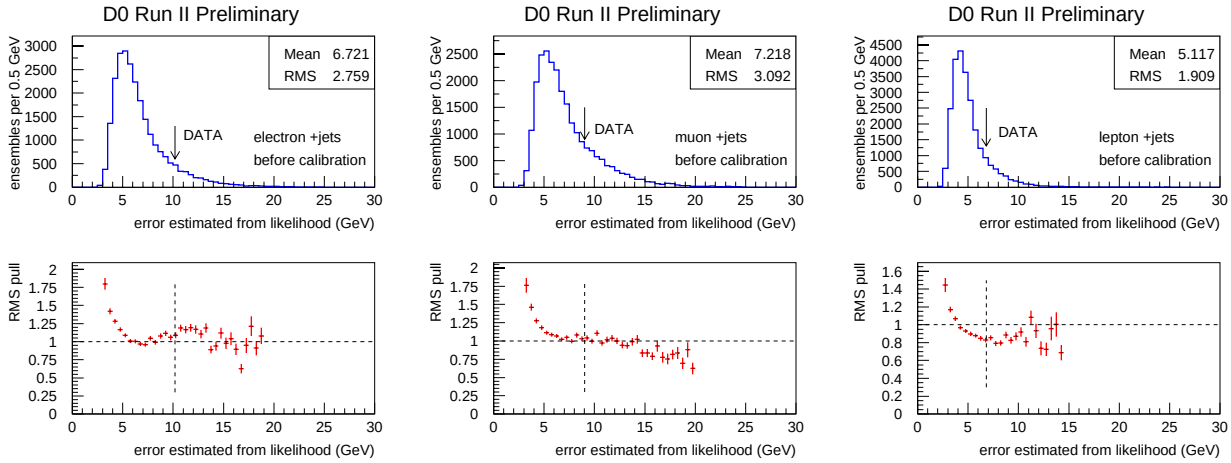

FIG. 12: Distributions of estimated statistical uncertainties and corresponding RMS width of the pull for the e+jets channel (left), μ+jets (middle) and the channels combined (right). For each channel the distribution was obtained from 25,000 simulated experiments at 175 GeV. In these plots the estimated uncertainty is not yet corrected for pull and calibration slope. The values obtained in the data are indicated by arrows.

for μ+jets, giving a combined result

$$m_{\rm t} = 177.5 \pm 5.8 \text{ (stat) GeV}$$

if only statistical uncertainties are taken into account. The estimated uncertainties obtained from data are compared to the expected uncertainties in Fig. 12.

D. Systematic uncertainties

Systematic uncertainties are evaluated in a similar way as for the Template analysis using ensemble tests. The uncertainty due to jet energy scale calibration and jet resolutions was determined by varying the corrections by one standard deviation up and down.

The uncertainty due to the trigger was determined by varying the trigger turn-on curves within their uncertainties. The underlying event and multiple interaction uncertainty reflects the difference in measured top quark mass between the nominal MC ensembles and the ensembles with the underlying event generation turned on. The MC statistics uncertainty reflects the statistical uncertainty in the determination of the bias from the calibration curve. The uncertainty due to the background level is the difference between ensembles with the nominal background contamination and ensembles without any background contamination. The background shape was varied by using different samples

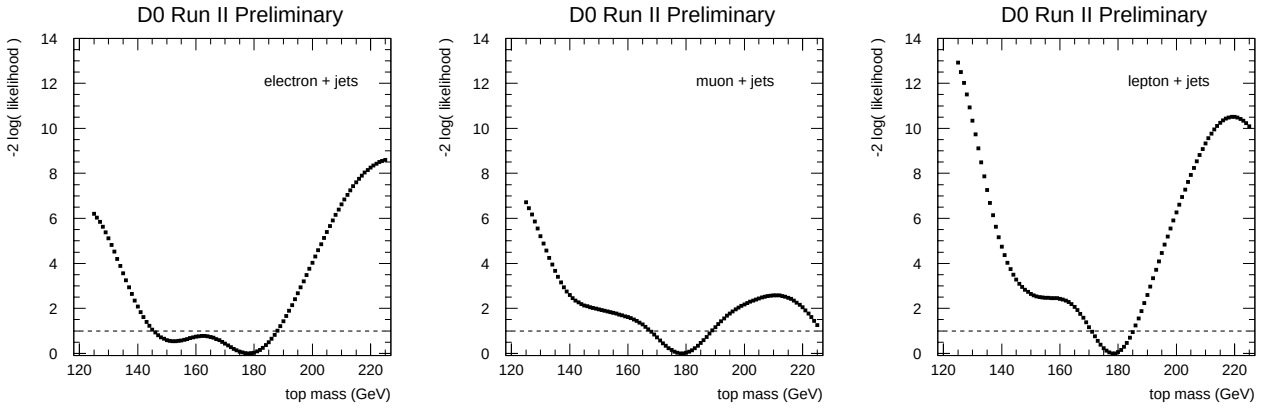

FIG. 13: Mass likelihood curves for the events observed in data, for e+jets (left), μ+jets (middle), and both channels combined (right). These likelihood curves are shown before calibration. At each value of the top mass the signal fraction is allowed to float freely in the likelihood fit.

Source	Uncertainty
Jet Energy Scale	-5.0 $+4.6$ GeV
Jet Energy Resolution	± 1.0 GeV
Trigger Uncertainty	± 0.5 GeV
Underlying Event and Multiple Interactions	$+1.8$ GeV
Limited MC Statistics	± 0.3 GeV
Noise/MI	± 2.6 GeV
Background Level	± 0.8 GeV
Background Shape	± 1.4 GeV
$t\bar{t}$ modeling	± 3.8 GeV
total	-7.1 $+7.0$ GeV

TABLE IV: Systematic uncertainties (preliminary) for the Ideogram analysis in the lepton+jets channel. See description in text.

of simulated W+jets events and multijet background samples from collider data. The uncertainties for the $t\bar{t}$ model and noise/multiple interactions are taken from the Run I top mass measurement. They were doubled to cover the possibility that the new analysis may have different sensitivities.

Preliminary values for the systematic uncertainties are summarized in Table IV. The combined systematic uncertainty is calculated by adding each of the uncertainties in quadrature.

VIII. CONCLUSION

In Table V, we summarize the results for the top quark mass using both the Template and the Ideogram techniques. For comparison, we performed both the Ideogram and Template fits with and without constraining the fitted signal fraction. As shown in Table V the agreement between the mass results is excellent when the purity is constrained to the expected value.

analysis	calibrated mass result
Template with constraint	170.0 ± 6.5 GeV
Template without constraint	172.1 ± 7.5 GeV
Ideogram, purity fixed to expectation	170.0 ± 9.4 GeV
Ideogram without constraint	177.5 ± 5.8 GeV

TABLE V: Mass results on the ℓ+jets data sample with and without purity constraint. Uncertainties are statistical only.

In conclusion, we present a preliminary measurement of the mass of the top quark in the lepton+jets channel based on an integrated luminosity of about 160 pb^{-1} of data from Run II of the Tevatron. Using two different techniques we measure

$$m_{\rm t} = 170.0 \pm 6.5({\rm stat}) \, ^{+10.5}_{-6.1} ({\rm syst}) \ {\rm GeV} \ ({\rm from \ Template \ method})$$

and

$$m_t = 177.5 \pm 5.8({\rm stat}) \pm 7.1({\rm syst}) \ {\rm GeV} \ ({\rm from \ Ideogram \ method}).$$

The range in the obtained values is mostly due to the different assumptions made in the background model. Figure 14 shows a plot comparing these results to previously published measurements.

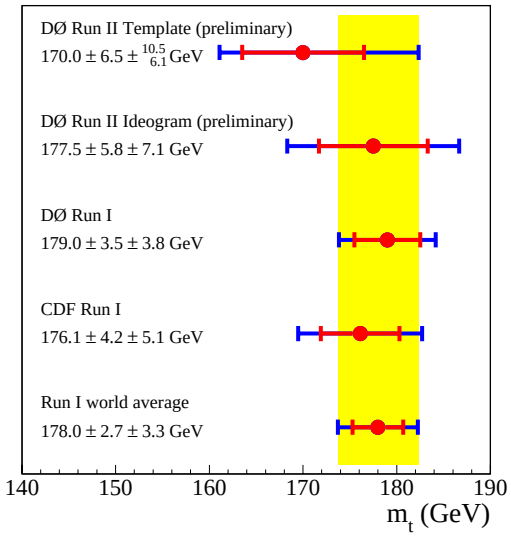

FIG. 14: The results from this paper compared to previous measurements of the top quark mass.

[1] CDF Collaboration, F. Abe *et al.*, Phys. Rev. Lett. **74**, 2626 (1995);
DØ Collaboration, S. Abachi *et al.*, Phys. Rev. Lett. **74**, 2632 (1995).
[2] DØ Collaboration, V.M. Abazov *et al.*, Nature **429**, 638 (2004).
[3] DØ Collaboration, B. Abbott *et al.*, Phys. Rev. D **58**, 052001 (1998)
[4] V. Barger and R. Phillips, *Collider Physics*, Addison-Wesley, NY, 1987
[5] DELPHI Collaboration, Eur. Phys. J. **C2**(1998) 581;
M. Mulders (DELPHI Collaboration), Int. J. Mod. Phys. A **16S1A** (2001) 284;
M. Mulders, Ph.D. thesis (FOM, Amsterdam & Amsterdam U.), Sep 2001, 226pp.